ELSEVIER

Effects of annealing on microstructure and electrochemical properties of the low Co-containing alloy Ml(NiCoMnAlFe)$_5$ for Ni/MH battery electrode

Zhi-Hong Ma [a], Ju-Feng Qiu [b,*], Li-Xin Chen [c], Yong-Quan Lei [c]

[a] *Baotou Hengyitong Rare Earth Co. Ltd., Hayenaobao Village, Jiuyuan District, Baotou 014060, PR China*
[b] *Baotou Research Institute of Rare Earths, No. 129, Tuanjie Street, P.O. Box 131, Baotou 014010, PR China*
[c] *Department of Materials Science and Engineering, Zhejiang, University, Hangzhou 310027, PR China*

Abstract

In this paper, an investigation has been made on the effects of the annealing at 1273 K for 7 h on the microstructure and electrochemical properties of the low Co-containing hydrogen storage alloy MlNi$_{3.8}$Co$_{0.3}$Mn$_{0.3}$Al$_{0.4}$Fe$_{0.2}$ for nickel/metal hydride (Ni/MH) battery electrode. X-ray diffraction (XRD) analysis and metallographic examinations show that annealing has no significant effect on the phase constituent and structure of the alloy, but can make the crystal lattice strain and composition segregation decrease, the dendrite structure disappear and the crystalline grain grow. The annealing at 1273 K for 7 h causes an increase in the maximum discharge capacity of the alloy electrode. Annealing can also bring about a decrease in the plateau potential and a considerable increase in the cycling stability of MlNi$_{3.8}$Co$_{0.3}$Mn$_{0.3}$Al$_{0.4}$Fe$_{0.2}$ alloy electrode. The mechanism of the improvement in the cycling stability was discussed based on the alloy crystallographic structure and microstructure change due to annealing.
© 2003 Elsevier B.V. All rights reserved.

Keywords: Rare earth; Hydrogen storage alloy; Annealing; Microstructure; Electrochemical property

1. Introduction

The mischmetal-based hydrogen storage alloy MmNi$_5$ has been used extensively as the negative electrode materials of the rechargeable nickel/metal hydride (Ni/MH) batteries because they possess the excellent characteristics of high energy storage density and cycling life [1,2]. The partial substitution of nickel with such elements as cobalt, manganese, aluminum, etc. in the MmNi$_5$ alloy can improve the corrosion resistance and charge–discharge cycling stability of the hydrogen storage alloy electrode. Among the substituting elements, cobalt has the prominent role, but it is expensive and its cost takes up more than one third of the total cost of the alloy raw materials, this makes the cost of commercially used alloy MmNi$_{3.55}$Co$_{0.75}$Mn$_{0.4}$Al$_{0.3}$ still higher [3]. Therefore, the research and development of MmNi$_5$ alloy with low Co content and high cycling stability is of interest not only for consumer batteries but also for electric vehicle applications. Recently, many investigations

have been made on the battery performance of Co-less and Co-free AB$_5$ type hydrogen storage alloy electrodes [4–16]. A few of reports have suggested that heat treatment can improve the composition homogeneity, decrease the crystal lattice strain and defect, thereby increase the discharge capacity and cycle life of the hydrogen storage alloy [17,18].

In this work, an MlNi$_{3.8}$Co$_{0.3}$Mn$_{0.3}$Al$_{0.4}$Fe$_{0.2}$ alloy (Ml denotes La-rich mischmetal) was prepared and annealed at 1273 K for 7 h in order to study the effects of annealing heat treatment on the microstructure and electrochemical properties such as activation, discharge capacity and cycle stability of the hydrogen storage alloy with low Co content.

2. Experimental

2.1. Preparation and characterization of the alloy

The low Co-containing MlNi$_{3.8}$Co$_{0.3}$Mn$_{0.3}$Al$_{0.4}$Fe$_{0.2}$ alloy was prepared by arc melting in a water-cooled copper crucible under an argon atmosphere. Each hearth alloy was re-melted three times to insure composition homogeneity.

* Corresponding author. Tel.: +86-472-2137535;
fax: +86-472-5152008.
E-mail address: profqiu@hotmail.com (J.-F. Qiu).

The composition of the lanthanum-rich mischmetal used in this study was La 56.0%, Ce 31.2%, Pr 3.1% and Nd 9.7% (mass fraction). The purity of the other metal raw materials was higher than 99.0%. The annealing was carried out in a vacuum heating furnace under a pressure of 4×10^{-3} MPa at 1273 K for 7 h. Some of the as-cast and annealed alloy buttons were crushed and ground mechanically into powder below 200 mesh. The prepared alloy powder was used for X-ray diffraction (XRD) analysis and fabrication of electrode for the electrochemical experiment. The rest of the alloy buttons were used for microstructure observation.

The crystallographic structure and phase identification was conducted using XRD 98 type X-ray diffractometer operated at 40 kV, 25 mA, $20° \leq 2\theta \leq 90°$ and Cu Kα radiation. The microstructure and morphology observation was made using S-570 type scanning electron microscope (SEM) and Leica DML type optical microscope. The segregation of the constituent elements in the alloy was examined by electron probe microanalysis (EPMA).

2.2. Electrochemical experiments

About 150 mg of the alloy powder was mixed with the electrolytic copper powder in the mass ratio of 1:2. The powder mixture was filled in a die and pressed into a diameter 10 mm sheet under a pressure of 1000 MPa at ambient temperature. The pressed sheet was sandwiched between two nickel foam plates and then welded a nickel ribbon as connection of the metal hydride electrode.

The electrochemical properties of the prepared electrode were determined in an open cell containing 6 mol/dm^3 KOH

Table 1
Lattice parameters and FWHM of MlNi$_{3.8}$Co$_{0.3}$Mn$_{0.3}$Al$_{0.4}$Fe$_{0.2}$ alloy

Alloy condition	a (nm)	c (nm)	V (nm^3)	c/a	FWHM
As-cast	0.50128	0.40592	0.088335	0.80977	0.42
Annealed	0.50165	0.40565	0.088406	0.80663	0.36

electrolyte solution at room temperature. In addition to the working electrode prepared by the metal hydride, the nickel hydroxide (NiOOH/Ni(OH)$_2$) and Hg/HgO was used as the counter electrode and the reference electrode, respectively. The electrochemical measurements were performed using a DC-5 type computer-controlled battery tester.

3. Results and discussion

3.1. Effect of annealing on the crystallographic structure and microstructure

XRD patterns of the as-cast and annealed MlNi$_{3.8}$Co$_{0.3}$Mn$_{0.3}$Al$_{0.4}$Fe$_{0.2}$ alloy are shown in Fig. 1. The lattice parameters and the full width at half of the maximum (FWHM) of the highest (1 1 1) peak are summarized in Table 1. From XRD data, it is revealed that MlNi$_{3.8}$Co$_{0.3}$Mn$_{0.3}$Al$_{0.4}$Fe$_{0.2}$ alloy consists of the matrix phase having the hexagonal CaCu$_5$-type structure and small quantities of the precipitated phase of La$_2$Ni$_7$. It appears that the annealing carried out at 1273 K for 7 h has no significant effect on the phase constituent and structure of the alloy, but decreases the amount of the second phase La$_2$Ni$_7$ in MlNi$_{3.8}$Co$_{0.3}$Mn$_{0.3}$Al$_{0.4}$Fe$_{0.2}$
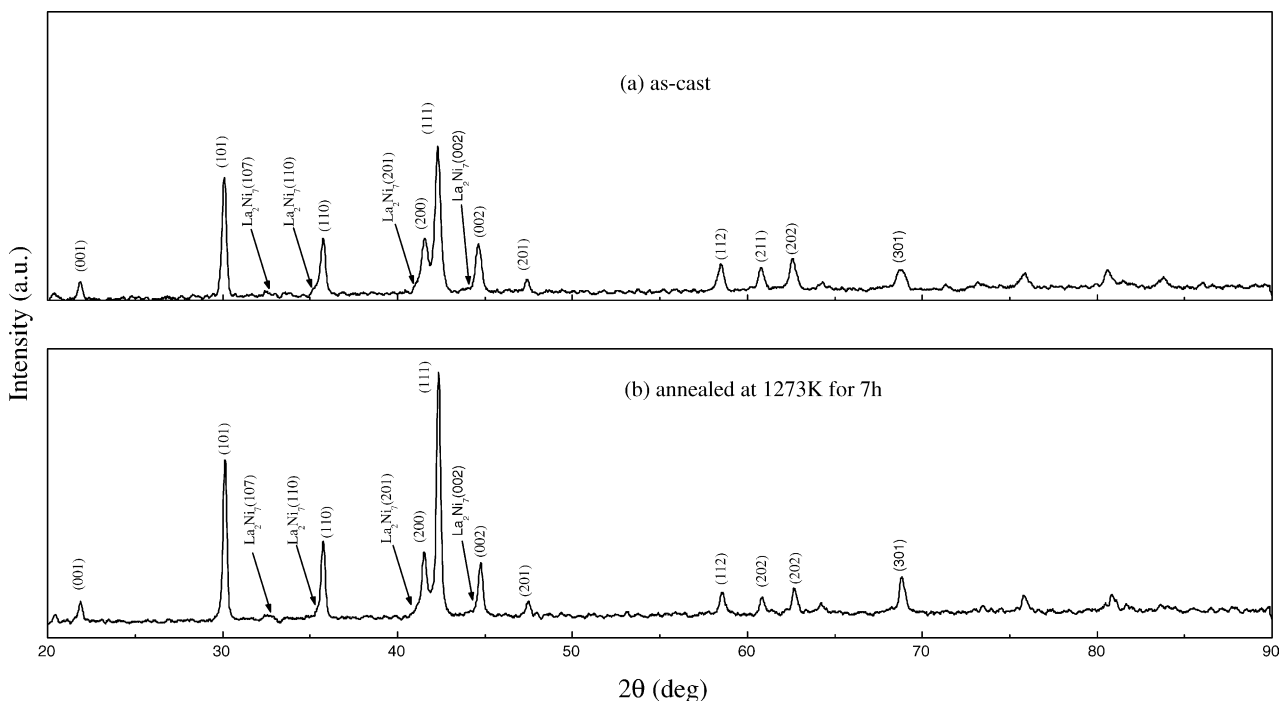
Fig. 1. XRD patterns of the as-cast (a) and annealed (b) MlNi$_{3.8}$Co$_{0.3}$Mn$_{0.3}$Al$_{0.4}$Fe$_{0.2}$ alloy.

alloy. From Table 1, we can see that annealing makes the alloy lattice parameters change, in particular, axis ratio (c/a) decrease remarkably, this may be related to the element substitution and distributing homogenization induced by the atom diffusion during annealing. From Fig. 1b and Table 1, it can be noted that XRD peaks became sharper after annealing of the alloy, the FWHM of the most intensive peak (1 1 1) reduced from 0.42 for the as-cast alloy to 0.36 for the annealed alloy, indicating that annealing can induce the release of crystallographic lattice strain and the growth of crystalline grain.

Fig. 2 shows the microstructures of the as-cast and annealed $MlNi_{3.8}Co_{0.3}Mn_{0.3}Al_{0.4}Fe_{0.2}$ alloy. It is very evident that the as-cast alloy displays the fine dendrite structure, which arranges in good order (Fig. 2a). After annealing at 1273 K for 7 h, the dendrite structure disappears and crystalline grain becomes large and non-uniform in size (Fig. 2b). It can be also seen that there are still small amounts of the second phase in the annealed alloy sample, it is in agreement with the result obtained by XRD analysis.

The distributions of the constituent elements such as La, Ni, Co, Mn, Al and Fe in the alloy were examined by EPMA. The results show that the considerable segregation of the constituent elements, especially La and Ni, occurs in the as-cast alloy. After annealing at 1273 K for 7 h, the segregation of the elements La and Ni, etc. decreases remarkably.

3.2. Effect of annealing on the electrochemical properties of the metal hydride electrode

3.2.1. Activation property and discharge capacity

The activation test was performed by charging at 60 mA/g for 7 h, resting for 10 min and then discharging at 60 mA/g down to −0.60 V with respect to Hg/HgO electrode. The
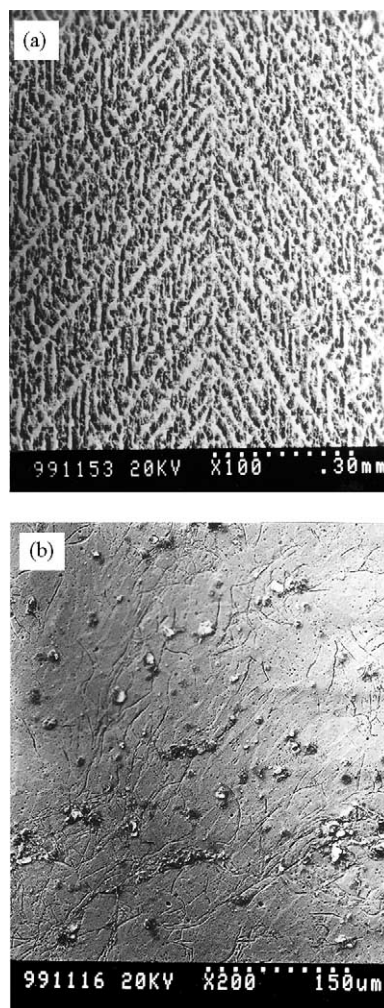

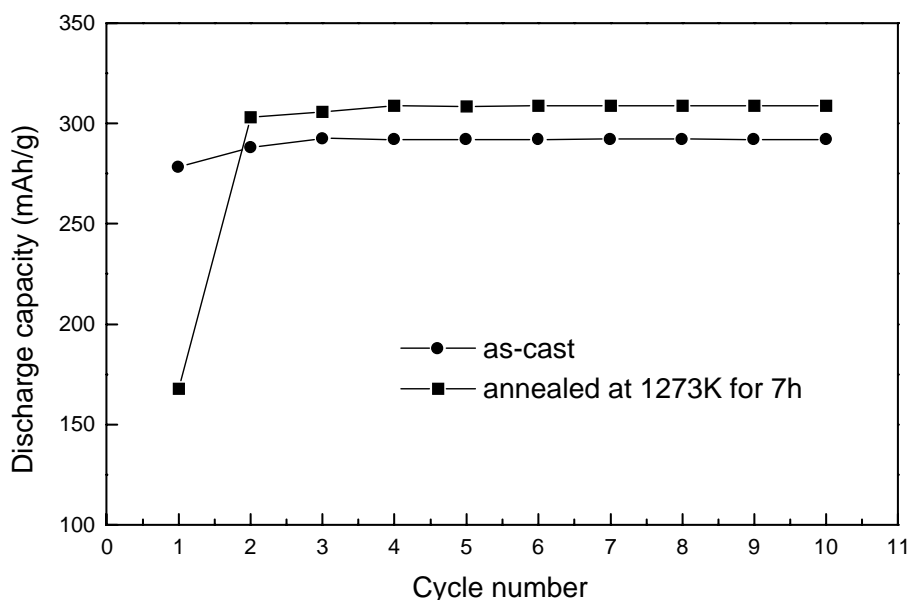Fig. 2. SEM micrographs of the as-cast (a) and annealed (b) $MlNi_{3.8}$-$Co_{0.3}Mn_{0.3}Al_{0.4}Fe_{0.2}$ alloy.

Fig. 3. Activation curves of the as-cast and annealed $MlNi_{3.8}Co_{0.3}Mn_{0.3}Al_{0.4}Fe_{0.2}$ alloy electrodes.
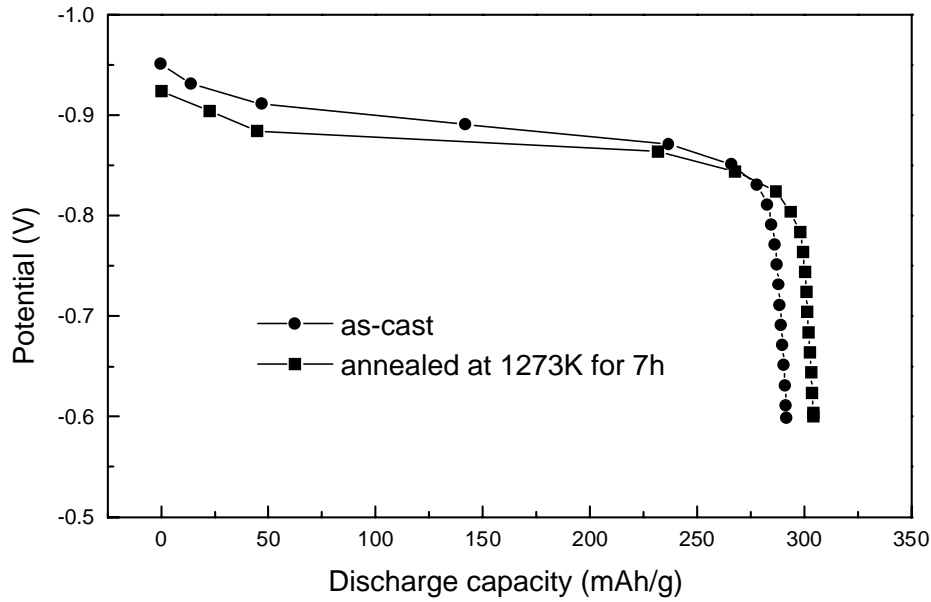
Fig. 4. Potential as a function of discharge capacity for the alloy electrodes.

activation curves of the electrodes made of the as-cast and annealed $MlNi_{3.8}Co_{0.3}Mn_{0.3}Al_{0.4}Fe_{0.2}$ alloy powder are shown in Fig. 3. We can see that the initial discharge capacity of the annealed alloy electrode was lower than that of the as-cast alloy electrode. The maximum discharge capacity (C_{max}) reached after three cycles for the as-cast alloy electrode and after four cycles for the annealed one, respectively, C_{max} of the latter (309 mAh/g) was higher than that of the former (292 mAh/g).

3.2.2. Plateau potential of discharge

Fig. 4 displays the effect of annealing on the plateau potential and slope of discharging potential at 60 mA/g

discharge current. It can be noted that the plateau potential of the annealed alloy electrode lowered to −0.876 V from −0.891 V for the as-cast one and the slope also lowered, i.e. the plateau became leveler. This could ascribe to the alloy composition homogenization induced by annealing [19].

3.2.3. Cycle stability of the alloy electrode

The charge–discharge cycle test was conducted by charging at 300 mA/g for 72 min, resting for 5 min and then discharging at 300 mA/g down to −0.60 V with respect to Hg/HgO electrode. The measured discharge cycle curves of the as-cast and annealed alloy electrodes are shown in Fig. 5.
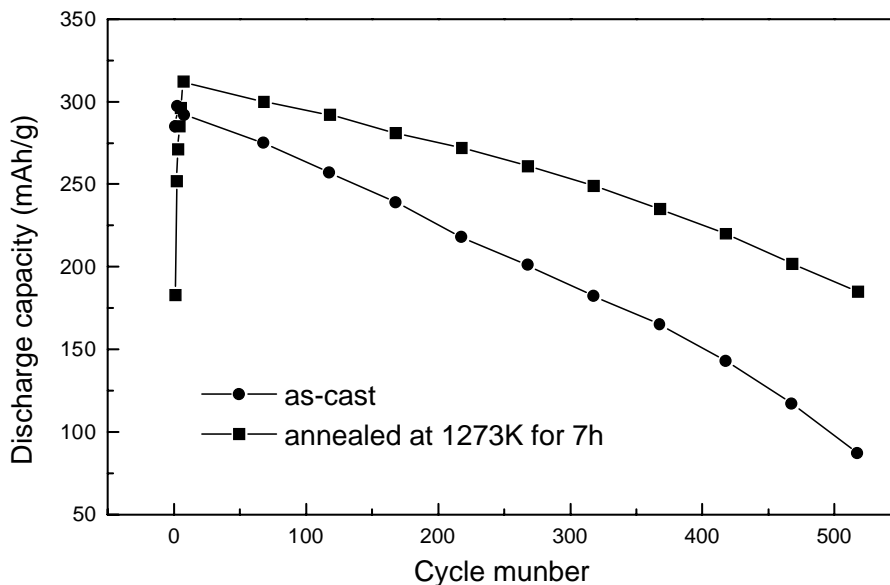

Fig. 5. Discharge cycling curves of the $MlNi_{3.8}Co_{0.3}Mn_{0.3}Al_{0.4}Fe_{0.2}$ alloy electrodes.
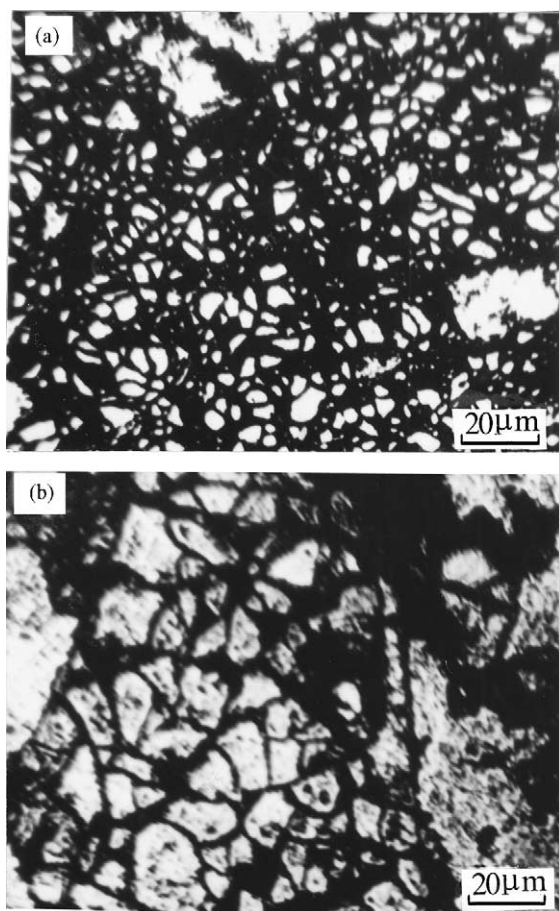
Fig. 6. Optical micrographs of the as-cast (a) and annealed (b) alloy electrode pellets after 514 cycles.

It can be noted that the retention rate of discharge capacity is 30% for the as-cast alloy electrode and 61% for the annealed one after 514 cycles, i.e. the cycling stability of the annealed alloy electrode increases by a factor of 2 as compared with the as-cast alloy electrode. The optical micrographs of pellets of electrodes cycled 514 times are shown in Fig. 6. We can see that after 514 cycles the as-cast alloy electrode pulverized to smaller particles, while the annealed alloy electrode pulverized to larger particles, indicating annealing can improve the pulverization and corrosion resistance, thereby the cycling stability of the alloy electrode.

The cycle stability of the mischmetal-based hydrogen storage alloy electrode closely correlates with the pulverization rate and corrosion resistance of the alloy electrode in KOH electrolyte solution [20]. As described above, the as-cast $MlNi_{3.8}Co_{0.3}Mn_{0.3}Al_{0.4}Fe_{0.2}$ alloy exhibited a dendrite structure (Fig. 2a), which was easy to absorb hydrogen and pulverize to particles, and the considerable composition segregation, which caused stoichiometric deviation toward the Ml-deficient side, resulting in significant capacity decay during cycling [21]. The annealing conducted at 1273 K for 7 h made the dendrite structure disappeared, crystalline grain grown, lattice strain released and the alloy composition ho-

mogenized. These effects of annealing could be important reasons for improving the corrosion resistance and lowering the pulverization rate of $MlNi_{3.8}Co_{0.3}Mn_{0.3}Al_{0.4}Fe_{0.2}$ alloy electrode.

4. Conclusions

The low Co-containing lanthanum-rich mischmetal-based hydrogen storage alloy $MlNi_{3.8}Co_{0.3}Mn_{0.3}Al_{0.4}Fe_{0.2}$ is composed of the matrix phase having a hexagonal $CaCu_5$-type structure and small amounts of the precipitate La_2Ni_7. The annealing performed at 1273 K for 7 h lowers quantity of the second phase of La_2Ni_7 and the crystal lattice strain. Furthermore, the typical dendrite structure in the as-cast alloy disappears, crystalline grain becomes large and segregation of La, Ni and Mn, etc. decreases upon annealing.

The annealing at 1273 K for 7 h causes an increase in the maximum discharge capacity of the alloy electrode. The plateau potential and slope of the annealed alloy electrode decrease, this attributes to the alloy composition homogenization induced by annealing. The cycling stability of $MlNi_{3.8}Co_{0.3}Mn_{0.3}Al_{0.4}Fe_{0.2}$ alloy electrode is increased considerably by annealing. Therefore, the cycling stability degradation due to decreasing Co content in the mischmetal-based alloy can be compensated by annealing.

References

[1] T. Sakai, T. Hazama, H. Miyamura, N. Kuriyama, A. Kato, H. Ishikawa, J. Less-Common Met. 172–174 (1991) 1175–1184.
[2] J.J. Reilly, G.D. Adzic, J.R. Johnson, T. Vogt, S. Mukerjee, J. McBreen, J. Alloys Comp. 293–295 (1999) 569–582.
[3] W.-K. Hu, H. Lee, D.-M. Kim, S.-W. Jeon, J.-Y. Lee, J. Alloys Comp. 268 (1998) 261–265.
[4] F. Meli, A. Züttel, L. Schlapbach, J. Alloys Comp. 231 (1995) 639–644.
[5] F. Lichtenberg, U. Köhler, A. Fölzer, N.J.E. Adkins, A. Züttel, J. Alloys Comp. 253–254 (1997) 570–573.
[6] G.D. Adzic, J.R. Johnson, S. Mukerjee, J. McBreen, J.J. Reilly, J. Alloys Comp. 253–254 (1997) 579–582.
[7] K. Yasuda, J. Alloys Comp. 253–254 (1997) 621–625.
[8] W.-K. Hu, D.-M. Kim, K.-J. Jang, J.-Y. Lee, J. Alloys Comp. 269 (1998) 254–258.
[9] M. Geng, J. Han, F. Feng, D.O. Northwood, J. Electrochem. Soc. 146 (1999) 2371–2375.
[10] P.H.L. Notten, M. Latroche, A. Perchero-Guégan, J. Electrochem. Soc. 146 (1999) 3181–3189.
[11] M. Geng, J. Han, F. Feng, D.O. Northwood, J. Electrochem. Soc. 146 (1999) 3591–3595.
[12] B. Deng, Y. Li, R. Wang, S. Fang, Electrochim. Acta 44 (1999) 2853–2857.
[13] M.M. Porović, B.N. Grgur, M.V. Vojnović, P. Rakin, N.V. Krstajić, J. Alloys Comp. 298 (2000) 107–113.
[14] C. Iwakura, K. Ohkawa, H. Senoh, H. Inoue, Electrochim. Acta 46 (2001) 4383–4388.
[15] C. Iwakura, K. Ohkawa, H. Senoh, H. Inoue, J. Electrochem. Soc. 149 (2002) A462–A465.

[16] P. Li, X.-L. Wang, Y.-H. Zhang, J.-M. Wu, R. Li, X.-H. Qu, J. Alloys Comp. 354 (2003) 310–314.

[17] T. Sakai, H. Yoshinaga, H. Miyamura, N. Kuriyama, H. Ishikawa, J. Alloys Comp. 180 (1992) 37–54.

[18] W.-K. Hu, D.-M. Kim, S.-W. Jeon, J.-Y. Lee, J. Alloys Comp. 270 (1998) 255–264.

[19] H. Nakamura, Y. Nakamura, S. Fujitani, I. Yonezu, J. Alloys Comp. 218 (1995) 216–220.

[20] J.J.G. Willems, Philips J. Res. 39 (1984) 54–70.

[21] T. Sakai, H. Miyamura, N. Kuriyama, H. Ishikawa, I. Uehara, Zeits. Physik. Chem. Bd. 183 (1994) 333–346.